Fracture behaviour of liquid crystal epoxy resin systems based on diglycidyl ether of 4,4′-dihydroxy-α-methylstilbene

Part II *Effect due to blending with TACTIX* 556 epoxy resin and phenolic monomers*

H.-J. SUE
Polymer Technology Center, Department of Mechanical Engineering, Texas A&M University, College Station, TX 77843-3123 USA

J. D. EARLS, R. E. HEFNER, Jr
Organic Product Research, B-1215, The Dow Chemical Company, Freeport, TX 77541 USA

The mechanical behaviours of unoriented, poured resin castings based on formulated blends containing the diglycidyl ether of 4,4′-dihydroxy-α-methylstilbene monomer are studied. It is found that the mechanical and fracture behaviours of these liquid crystalline epoxy (LCE) blends vary significantly. In general, the LCE blends possess much higher fracture toughness and fatigue crack resistance than conventional epoxy resins. At low temperatures ($-40\,^{\circ}C$), the K_{IC} values of the LCE blends are slightly higher than those measured at room temperature. The common fracture mechanisms observed in the ductile LCE blends are crack segmentation, crack branching, crack bridging and crack blunting. The fracture surfaces of the tougher LCE blends only exhibit limited ductile drawing (furrow pattern) at the slow crack growth region; no signs of shear lips on the edges of the starter crack region are observed. The optical microscopy and transmission electron microscopy work suggests that orientation and/or transformation toughening may be the source for such high fracture toughness of the LCE blends. The possible cause(s) of the unusual fracture behaviour of the LCEs is discussed. Approaches for making high performance LCE blends are also addressed.

1. Introduction

The fracture behaviours of pour-cast, unoriented, diglycidyl ether of 4,4′-dihydroxy-α-methylstilbene (DGE-DHAMS)/sulphanilamide liquid crystalline epoxy (LCE) resin systems cured under various temperatures were studied and reported in part I of this series [1]. It was shown that crack segmentation, crack branching, crack bridging, and crack deflection are among the major toughening mechanisms operative in the toughest LCEs. It was also shown that control of the LCE morphology is extremely important in tailoring their mechanical and fracture properties [2, 3]. There are also other important factors which may affect the mechanical performance of LCEs that remain to be addressed. Among the important factors to be investigated in this paper is the blending of the mesogenic DGE-DHAMS LCE with other experimental and commercially available epoxies and monomers.

The present study, which is part of a larger effort on fundamental understanding of the structure–property relationship for the LCE systems, focuses on the mechanical properties and fracture behaviour characterizations of DGE-DHAMS blended with the DHAMS monomer, TACTIX 556 (2.2 functional dicyclopentadiene epoxy novolac) resin, and the Novolac Resin to 3.6 functional phenolic novolac resin [4]. It is hoped that, as a result of this study, a better understanding can be achieved on how to tailor the LCE morphology, rheology, stiffness, glass-transition temperature (T_g), fatigue and fracture behaviour by mixing with other experimentally/commercially available epoxies and monomers. Issues concerning how the physical and mechanical properties of the LCEs can be altered by blending are addressed.

2. Experimental procedure

2.1. Materials

The chemical structures of DGE-DHAMS and sulphanilamide to be used in this study were given in part I of this series [1]. The general synthesis and

* Trademark of The Dow Chemical Company.

0022–2461

physical properties of the LCEs have also been described elsewhere [2, 3, 5–7]. Only the compositions and the curing conditions of the LCE blends to be studied in this work are given below.

Three LCE blends are utilized in this work. These LCE blends include (1) DGE-DHAMS : DHAMS : sulphanilamide ((1 : 0.4 : 0.6 ratio by equivalent weight (EW)), (2) DGE-DHAMS : DHAMS : phenolic novolac resin : sulphanilamide (1 : 0.4 : 0.5 : 0.1 ratio by EW) and (3) DGE-DHAMS : TACTIX* 556 epoxy resin : sulphanilamide (0.79 : 0.21 : 1.0 ratio by EW). It is noted that thephenolic epoxy novolac resin, and sulphanilamide are utilized as cross-linkers.

The curing conditions for the three blends are given as follows:

1. DGE-DHAMS/DHAMS/sulphanilamide: 4.25 h at 120 °C + 1 h at 140 °C + 1 h at 160 °C + 1 h at 180 °C + 4 h at 200 °C (Blend 1).
2. DGE-DHAMS/DHAMS/phenolic novolac resin/sulphanilamide: 4 h at 135 °C + 1 h at 150 °C + 1 h at 175 °C + 2 h at 200 °C (Blend 2).
3. DGE-DHAMS/Tactix* 556 epoxy resin/sulphanilamide: 4 h at 120 °C + 1 h at 140 °C + 1 h at 160 °C + 1 h at 180 °C + 4 h at 200 °C (Blend 3).

Blend 1 was chosen to give a high mesogenic backbone content in the system. Blend 2 was chosen for its low cross-link density, high matrix ductility and good "tack and drape" properties as prepreg materials [4]. While for Blend 3, it is expected that the high backbone rigidity of the Tactix* 556 epoxy resin will help provide increased stiffness and T_g.

2.2. Sample preparation

The unoriented LCE blends with plaque thicknesses of 0.635 cm and 0.3175 cm were cast and slowly cooled to room temperature (25 °C) in the oven. The 0.635 cm plaques were machined into bars with dimensions of $12.7 \times 1.27\,\text{cm} \times 0.635\,\text{cm}$ and dimensions of $6.35 \times 1.27 \times 0.635$ cm for the DN-4PB [8–10] and the single-edge-notch three-point-bend (SEN-3PB) [1, 11–13] experiments, respectively. The detailed sample preparation and testing procedures for the DN-4PB and SEN-3PB experiments have already been given in part I of this series [1].

The 0.3175 cm plaques were cut into bars with dimensions of $15.24 \times 2.54 \times 0.3175$ cm for SEN tension (SENT) fatigue crack propagation tests [14, 15] and dimensions of $6.35 \times 1.27 \times 0.635$ cm for both DMS and 3PB-F tests. The sharp notch of the SENT specimen was prepared the same way as that of the SEN-3PB specimens. An a/W (crack length to specimen width) ratio of about 0.2 was used for the SENT experiment.

2.3. Dynamic mechanical spectroscopy (DMS)

To determine the relationship of the modulus of the LCEs as a strong function of temperature, the dynamic mechanical behaviour of Blend 2 was studied using DMS (Rheometrics RMS-805) under a torsional mode, with 5 °C per step. A constant strain amplitude of 0.05% and a fixed frequency of 1 Hz were used. The sample was analysed at temperatures ranging from − 150 °C to 200 °C. For comparison purposes, the DMS of an equivalently formulated tough epoxy resin (DGEBA epoxy, phenolic novolac and sulphanilamide) [4] was also obtained.

2.4. Mechanical properties characterization

A Sintech-2 screw-driven mechanical testing machine was used to conduct the room temperature DN-4PB, SEN-3PB, and 3PB-F experiments. To ensure a valid K_{IC} measurement, cross-head speeds of $0.508\,\text{cm}\,\text{min}^{-1}$, $0.508\,\text{cm}\,\text{min}^{-1}$, and $0.0508\,\text{cm}\,\text{min}^{-1}$ were utilized to conduct the SEN-3PB experiments for Blend 1, Blend 2 and Blend 3, respectively.

For the 3PB-F experiment, a cross-head speed of $0.125\,\text{cm}\,\text{min}^{-1}$ was adopted. The flexural modulus was calculated based on the ASTM D790 method. For the low temperature (− 40 °C) K_{IC} and flexural modulus measurements, the materials testing system (MTS) servo-hydraulic 55 KIP (24.44 t) system with an environmental chamber was used to conduct the SEN-3PB and the 3PB-F experiments. The DN-4PB experiment was conducted according to part I of this series [1].

In the room temperature (25 °C) fatigue crack propagation experiment, a materials testing system servo-hydraulic 55 KIP (24.44 t) system (Model 810.13) with an MTS 445 controller was used. The fatigue test was performed at 1 Hz with a constant sinusoidal load amplitude and with a R-ratio, i.e. minimum load divided by maximum load, of 0.1. The sinusoidal waveform was generated using the MTS Model 436 control unit. The linear elastic fracture mechanics (LEFM) method, i.e. $\mathrm{d}a/\mathrm{d}N$ versus ΔK (increment of the crack advancement, a, per fatigue cycle, N, versus difference between the maximum and minimum stress intensity factor), was utilized to characterize the stable fatigue crack propagation region (Paris law region [15]) of the LCE blends. Detailed procedures for obtaining the $\mathrm{d}a/\mathrm{d}N$ versus ΔK data can be found elsewhere [14, 15].

2.5. Microscopy

The detailed procedures for preparing transmission electron microscopy (TEM) and transmission optical microscopy (TOM) samples of the damage zone around the survived DN-4PB crack in this study were the same as those described in part I of the series [1].

For the reflected OM (ROM) experiment, the plane strain core region was polished following the procedure described by Sue *et al.* [10]. The thin sections as well as the polished surface of the damage zone were then studied using an Olympus Vanox-S microscope both under bright field and cross-polarization conditions. The fracture surfaces of the LCE blends from the SEN-3PB specimens were studied using a Jeol JSM-IC845A scanning electron microscope (SEM), operating at an accelerating voltage of 20 kV. The

SEM samples were coated with 20 nm of Pd–Au to minimize charging.

3. Results and discussion

The present study intends to convey the concept and utility of blending experimental and commercial epoxies and phenolic monomers with the DGE-DHAMS LCE to obtain a spectrum of new LCE systems for a wide range of applications. The basic characterization of the physical and mechanical properties of these LCE blends are therefore needed. The present study focuses on investigating the mechanical properties of these potential LCE blends.

3.1. Dynamic mechanical spectroscopy

To determine the strong temperature dependency of the LCE modulus, in comparison with conventional epoxies, the DMS spectra of Blend 2 as well as a formulated tough epoxy resin [4] were generated. As shown in Fig. 1, the shear storage modulus (G') of Blend 2 clearly exhibits a much stronger temperature dependency than that of the formulated tough epoxy resin [4] over the entire temperature range investigated (except around the T_g region). At temperatures above $-20\,^{\circ}C$ up to the T_g of the tough epoxy, the G' of the tough epoxy resin is higher than that of Blend 2. Whereas, at temperatures below $-20\,^{\circ}C$, the G' of Blend 2 approaches that of the formulated epoxy resin. These data, therefore, indicate that if the service temperature is below $-20\,^{\circ}C$, the LCEs may possess either a similar or even a higher modulus than the tough epoxy resin. To verify this point, the 3PB-F experiment at $-40\,^{\circ}C$ was conducted, as reported below.

It is noted that the strong temperature dependency of the LCEs corresponds well to the relatively high magnitude of the tan δ (ratio between loss modulus and storage modulus) curve of LCEs. This, in turn, implies that the sub-T_g molecular motion in LCEs is much more pronounced than that of the conventional epoxies. Unfortunately, there is no known method that can be utilized to characterize the cross-link density of LCEs. As a result, it is uncertain if the temperature dependency of LCE modulus is due to incomplete curing of LCE or due to the nature of LC molecular packing. This issue will be tackled in the future.

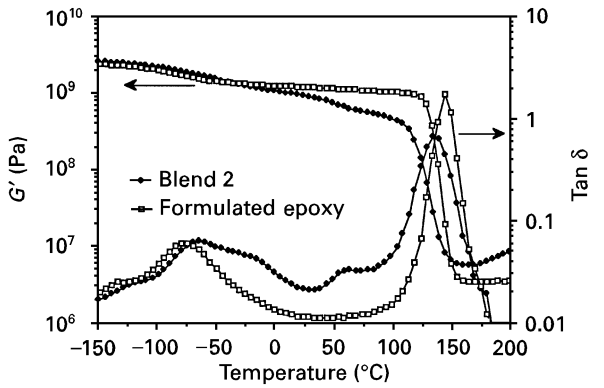

Figure 1 Dynamic mechanical spectra for Blend 2 (●) and the formulated tough epoxy resins (□) [4].

TABLE I Summary of the room temperature 3PB-flexural moduli and fracture toughness of the LCE blends

	E[a] (MPa)	K_{IC}[b] (MPa m$^{0.5}$)	G_{IC} (J m^{-2})	T_g[c] (°C)
Blend 1	2700	1.65 ± 0.10[d]	1080	180
Blend 2	2400	1.89 ± 0.04[d]	1310	135
Blend 3	3300	1.11 ± 0.08[e]	325	224[f]
Tough epoxy [4, 20]	3200	1.00 ± 0.10[e]	280	145

[a] 3PB-flexural moduli measured at 25 °C.
[b] The errors indicate the standard of deviation.
[c] Obtained from the primary tan δ peak of the dynamic mechanical spectrum.
[d] Cross-head speed = 0.508 cm min^{-1} and measured at 25 °C.
[e] Cross-head speed = 0.05 cm min^{-1} and measured at 25 °C.
[f] Obtained from [2].

TABLE II Summary of the low temperature ($-40\,^{\circ}C$) 3PB-flexural moduli and fracture toughness of the LCE blends

	E[a] (MPa)	K_{IC} (MPa m$^{0.5}$)	G_{IC} (J m^{-2})
Blend 1	4000	2.23[b,c]	1080
Blend 2	3400	1.89[b,c]	900
Blend 3	–[d]	1.13 ± 0.08[b]	–[d]
Tough epoxy [4, 20]	3700	1.07 ± 0.10[b]	270

[a] 3PB-flexural moduli measured at $-40\,^{\circ}C$ [2].
[b] Crosshead speed = 0.508 cm min^{-1}.
[c] Only three specimens tested.
[d] Not measured.

3.2. Mechanical properties

3.2.1. Three-point-bend flexural modulus measurement

Owing to the simplicity of the sample preparation and experimental procedures, the 3PB-F experiment was chosen to measure the modulus of the LCE blends, both at room temperature (25 °C) and at $-40\,^{\circ}C$.

The flexural moduli of the three unoriented LCE blends are either about the same or lower than that of the formulated tough epoxy resin at room temperature (Table I). However, when the test is conducted at $-40\,^{\circ}C$, the moduli of the LCEs become higher (Table II). The largest increase in flexural modulus from 2.7 GPa to 4.0 GPa is observed for the Blend 1 system where the concentration of the mesogenic segments is the highest. This suggests that if the temperature under which Blend 1 is to be utilized is below ambient temperature, then a higher modulus of the LCE can be anticipated.

3.2.2. Fracture toughness measurement

The SEN-3PB method was utilized for measuring the K_{IC} values of the LCE blends both at 25 °C and at $-40\,^{\circ}C$. The experimental procedure and the algorithm for obtaining K_{IC} as well as G_{IC} has been given elsewhere [11–13]. As shown in Tables I and II, both the K_{IC} and G_{IC} values of the LCE blends, either at 25 °C or at $-40\,^{\circ}C$, are higher than conventional epoxies [5, 8]. Furthermore, at low temperatures ($-40\,^{\circ}C$), the high fracture toughness of the LCE

blends is maintained at the room temperature level. These data therefore imply the potential utility of LCEs in cryogenic environments.

It should be noted that, as will be addressed in a separate paper, the fracture toughness of the LCEs is found to be a strong function of testing rate. In many cases, non-linear load–displacement curves before unstable fracture are observed in these LCEs, even though the fracture surface exhibits either brittle or semi-brittle characteristics, i.e. no signs of shear-lips or ductile drawing are observed. The fracture behaviours of the LCE blends are discussed in Section 3.3.

3.2.3. Fatigue crack propagation characterization

In the fatigue testing, care is taken to make sure a proper alignment of the SENT specimen with the loading frame is obtained. Also, depending on the fracture toughness of the individual LCE, the load level, i.e. ΔK, and the starter crack length are appropriately chosen so that the total fatigue cycles to failure is controlled to at least 2000 cycles and at most 10 000 cycles.

When the da/dN versus ΔK curves of the LCE blends are plotted, as shown in Fig. 2, the LCE blends exhibit much better fatigue crack propagation resistance curves than conventional diglycidyl ether of Bisphenol A (DGEBA) epoxy, i.e., DER* 332 epoxy resin, cured with 4,4′-diaminodiphenylsulphone. That is, the curves of the LCE blends are all located on the right-hand side of the conventional DGEBA epoxy curve. Furthermore, the formulated tough epoxy [4], Blend 1 and Blend 2 all appear to fall on the same curve before their individual unstable crack propagation ensues. The slopes for the curves of the conventional DGEBA epoxy, Blend 3 and the rest of the LCEs are 16, 10 and 6, respectively. Based on these results, it is clear that the LCE blends exhibit a much higher fatigue crack propagation resistance than most commercially available epoxies [17].

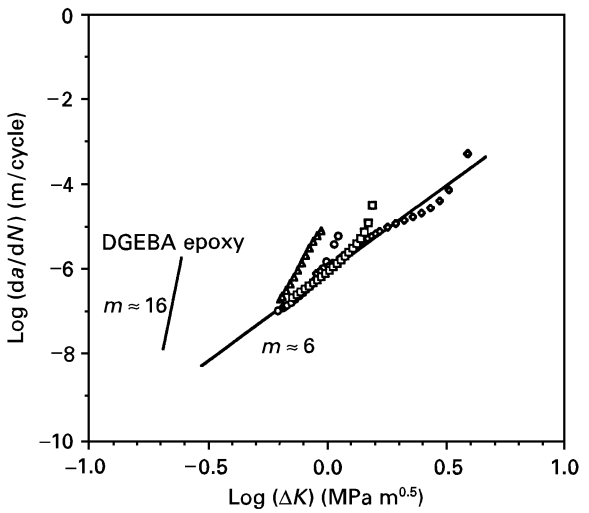

Figure 2 The da/dN versus ΔK plots of the LCE blends, the formulated tough epoxy [4], and a conventional DGEBA epoxy. (□) Blend 1; (◇) Blend 2; (○) formulated epoxy; (△) Blend 3. 1/Wz, $R = 0.1$, temperature 25 °C.

It is also noted that the ΔK level for the onset of unstable crack propagation for the LCE blends appears to correspond well with the K_{IC} of the individual resin, except for the Blend 2 system. This inconsistency may be partially due to the high rate-sensitivity of the fracture toughness of Blend 2 [18]. It is noted that for Blend 2, a higher testing rate results in a higher fracture toughness value [18].

3.3. Fracture mechanisms

The fracture toughness values of the LCE blends, as shown in Tables I and II, are significantly higher than conventional epoxies. Also, the previous paper [1] indicates that the major toughening mechanisms in the toughest LCE are crack segmentation, crack branching, crack deflection and crack bridging. In this study, since the ductility and the structure of the LCEs are altered by changing the formulation, it is conceivable that the high fracture toughness values observed in Blend 1 and Blend 2 may be the result of contributions by other failure mechanisms, in addition to the toughening mechanisms mentioned above. Therefore, the fracture mechanisms in the three LCE blends were studied in detail.

The fracture surfaces of all the LCE blends and the tough epoxy resin were first investigated using SEM. As shown in Figs 3–6, the fracture surface features in

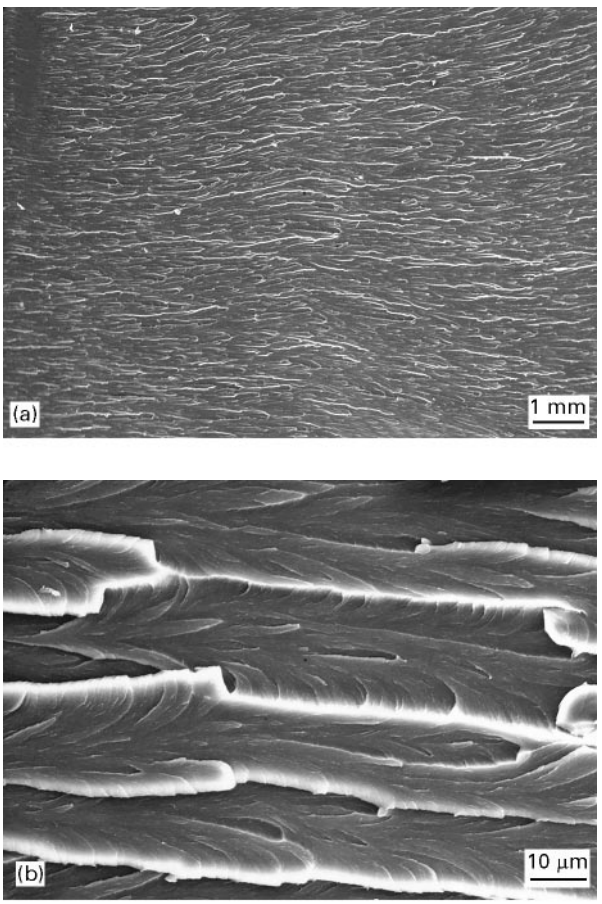

Figure 3 SEM micrographs showing the SEN-3PB fracture surface of Blend 1. The furrow pattern at the starter crack region is found to be much bigger and coarser than those of the conventional epoxies. (a) low magnification and (b) high magnification.

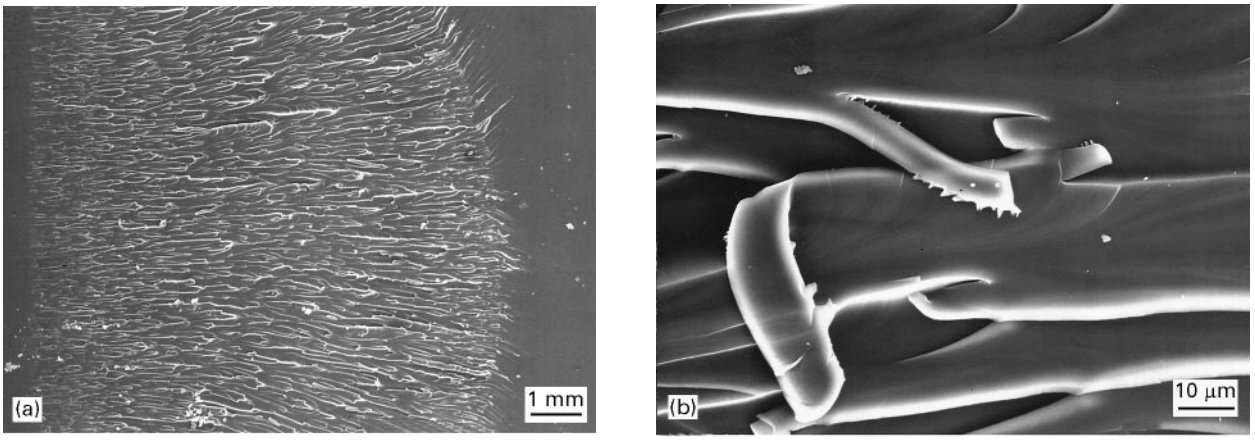

Figure 4 SEM micrographs showing the SEN-3PB fracture surface of Blend 2. The furrow pattern at the starter crack region is much bigger and coarser than those of the conventional epoxies. Signs of "hackling" appear to exist on the welt [16]. (a) low magnification and (b) high magnification.

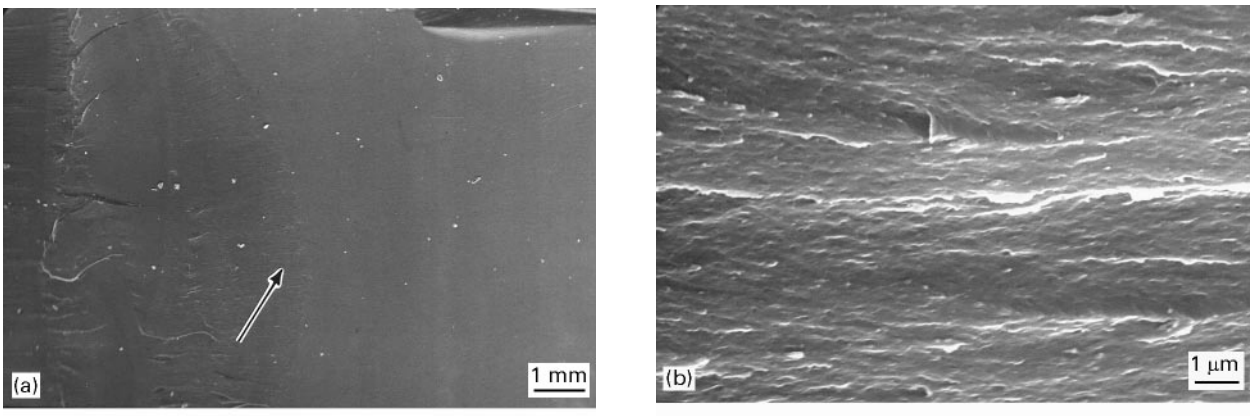

Figure 5 SEM micrographs showing the SEN-3PB fracture surface of Blend 3. The furrow pattern at the starter crack region (see arrow) is extremely small. (a) low magnification and (b) high magnification.

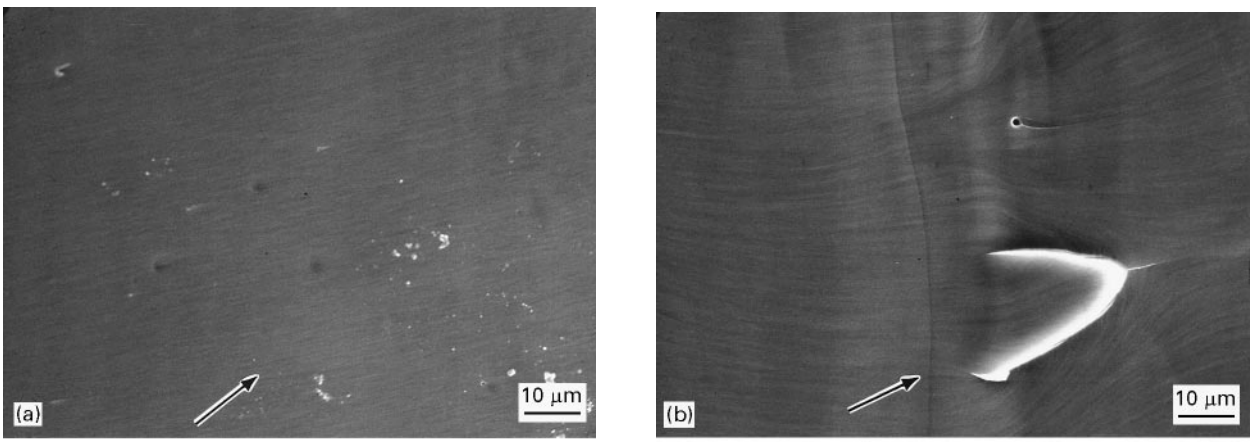

Figure 6 SEM micrographs showing the SEN-3PB fracture surface of the formulated tough epoxy resin. The furrow pattern, if any, at the starter crack region (see arrow) is extremely small. (a) low magnification and (b) high magnification.

these systems are quite similar, except that the size of the starter crack plastic zone (furrow region) is found to be much bigger for the higher fracture toughness LCEs. Surprisingly, for Blend 1 and Blend 2 systems which exhibit high K_{IC} values, no signs of shear-lip or plastic suck-in is present on their fracture surfaces (Figs 3 and 4). This implies that there must be other fracture mechanisms operating in the sub-fracture surface zone (SFSZ).

To effectively study the SFSZ of a damaged sample, it is desirable that the DN-4PB technique be used. Since both Blend 3 and the tough epoxy resin exhibit a brittle type of fracture behaviour with low K_{IC} values, they were not further investigated

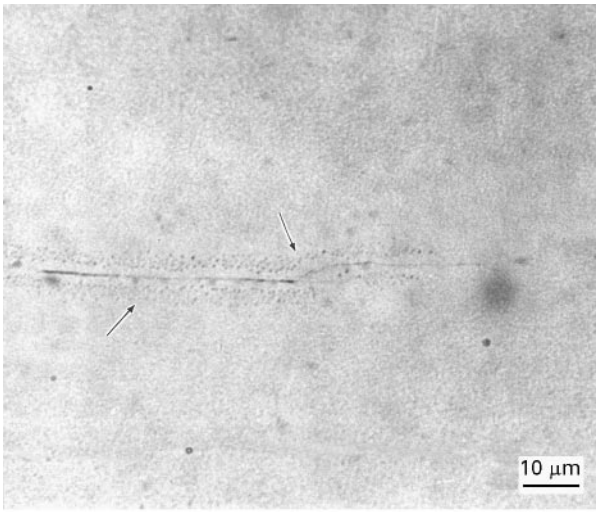

Figure 7 ROM bright field micrograph taken at the DN-4PB crack tip damage zone of Blend 1. A layer of transformation zone may be formed around the crack (see arrows).

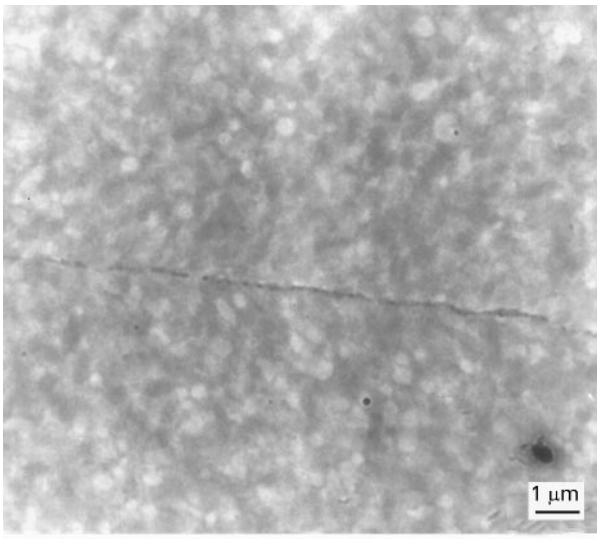

Figure 9 TEM micrograph taken (higher magnification than Fig. 8) at the DN-4PB crack tip of Blend 1.

here. Only Blend 1 and Blend 2 were studied in detail.

For the Blend 1 system, the sample is opaque and contains liquid crystallinity in the matrix. The observation of the SFSZ of Blend 1, using ROM, indicates that a highly localized transformation zone surrounds the crack (Fig. 7). This type of feature is analogous to the so-called transformation toughening in metal and ceramic fields. This transformation zone can be induced due to the change(s) of the crystalline structure, formation of microcracks, and rearrangement of the local domain orientation around the crack. A TEM investigation was undertaken to determine the possible cause(s) for such a feature.

When the TEM is utilized, it is evident that LC domains are present in Blend 1 (Figs 8–10). In the SFSZ, in addition to crack segmentation, crack bridging, crack bifurcation and crack deflection mechanisms observed in neat LCE matrices [1], the orientation and/or transformation toughening [19] may

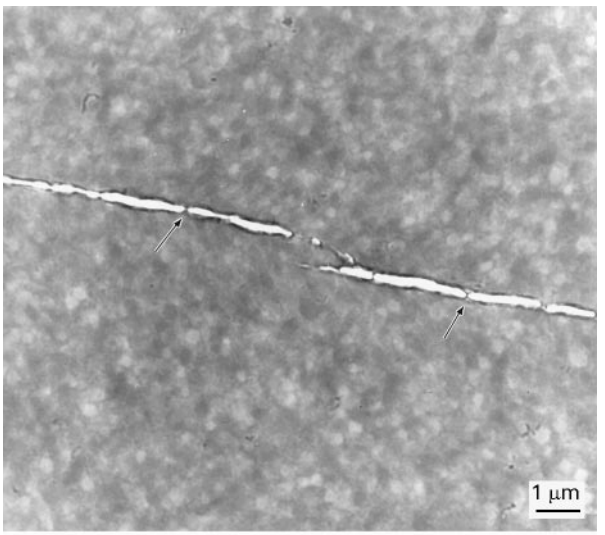

Figure 10 TEM micrograph taken at the DN-4PB crack wake of Blend 1. Crack bifurcation and crack segmentation are observed. When the main crack opens up, the matrix material between the segmented crack acts as a bridge (see arrows) to resist crack propagation.

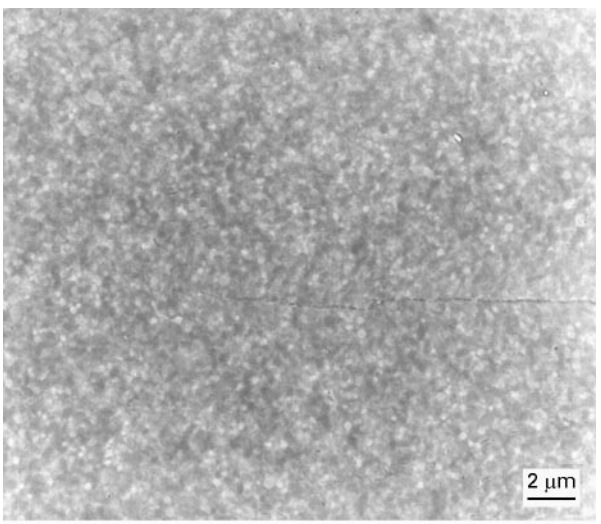

Figure 8 TEM micrograph taken at the DN-4PB crack tip of Blend 1. Signs of oriented LC domains and bridged crack are found.

be present in Blend 1. The LC domains around the crack tip and crack wake are found to be stretched at certain angles with respect to the crack plane. These angles vary from $\approx 45^\circ$ at the crack wake (Figs 9 and 10) to $\approx 90^\circ$ right in front of the crack tip (Fig. 8). The amount of LC domain stretching is found to be as much as 60%. This high degree of LC domain stretching may have induced LC structure transformation, which is evidenced in ROM (Fig. 7). Unfortunately, at this stage, we are unable to confirm LC structure transformation due to the lack of appropriate tools [1, 19]. The stretching (orientation) of the LC domains at the crack tip may help align the LC molecules to become perpendicular to the crack propagation direction. This LC molecular orientation may result in further crack propagation resistance of the LCE. In summary, the major toughening mechanisms operative in Blend 1 are found to be due to possible

orientation and/or transformation toughening, accompanied by the less effective crack bridging, crack segmentation, crack bifurcation and crack deflection mechanisms.

For the Blend 2 system, the bulk sample is translucent from visual observation. This suggests that Blend 2 either possesses extremely small LC domains that do not scatter light or that the matrix is amorphous in nature. When the SFSZ thin section with ≈ 40 μm thickness is viewed using TOM (Fig. 11), there appears to be the presence of morphological texture in the matrix, i.e. the granular texture shown in Fig. 11a and the birefringent pattern shown in Fig. 11b. A highly birefringent, yet localized, shear yielded zone is found around the crack inside the SFSZ. In addition, highly bifurcated cracks are observed both at the crack tip and at the crack wake (Fig. 11a and c). To further investigate the morphology and fracture mechanisms in Blend 2, a TEM investigation was conducted.

As shown in Figs 12–14, no signs of LC domains can be found using TEM. The SFSZ of this system is quite featureless, except for the presence of the apparent crack tip blunting (Fig. 13), crack segmentation (Fig. 14), crack bifurcation (Fig. 11) and crack bridging mechanisms (Figs 12–14). Owing to the homogeneity of the system, the crack deflection mechanism is not observed. Therefore, the major toughening mechanisms

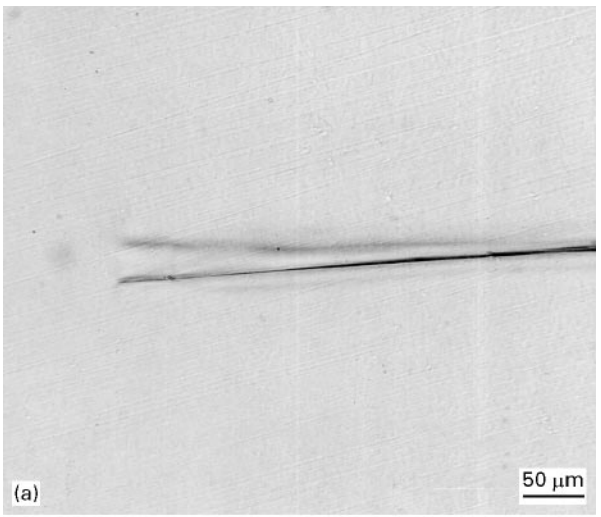

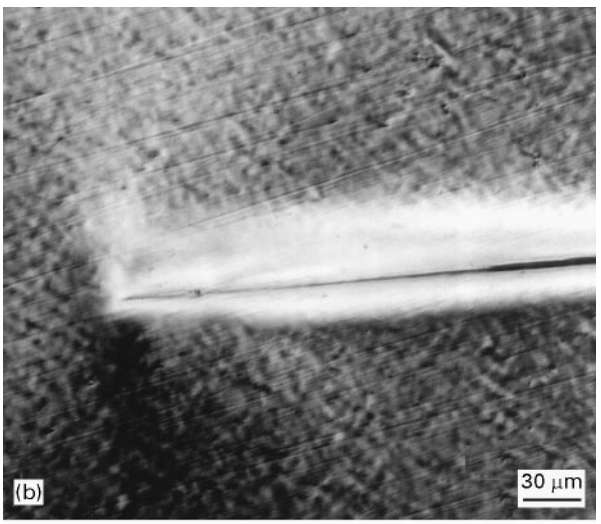

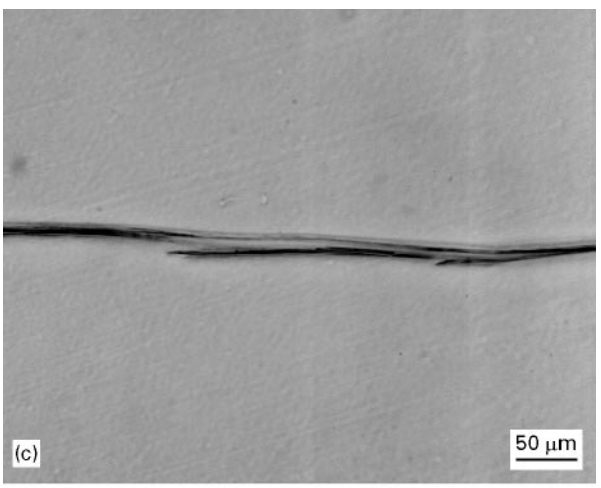

Figure 11 TOM micrographs of the DN-4PB damage zone of Blend 2 taken (a) under bright field, (b) under crossed-polars, and (c) at the crack wake (bright field). Matrix shear yielding and crack bifurcation are observed. Irregular birefringent pattern (in (b)), which may have resulted from local molecular orientation, in the matrix is also present.

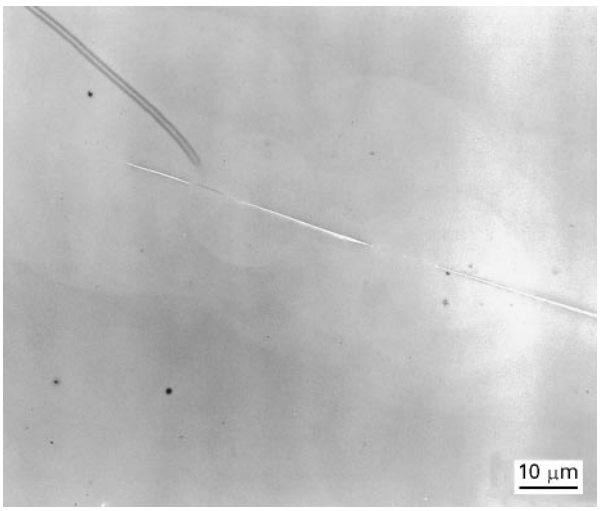

Figure 12 TEM micrograph taken at the DN-4PB crack tip damage zone of Blend 2. Crack segmentation is observed.

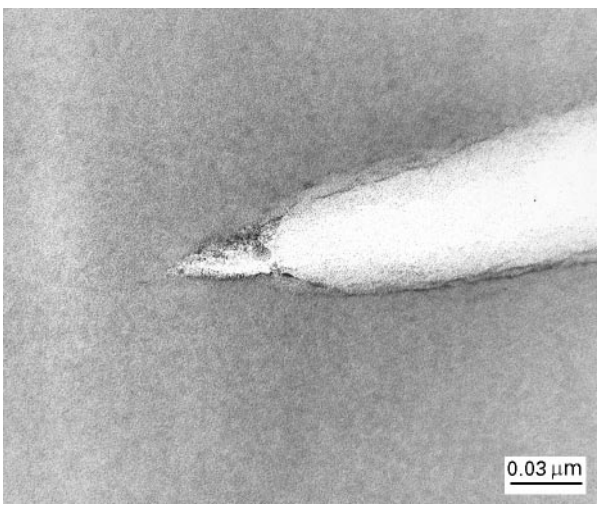

Figure 13 TEM micrograph taken at the DN-4PB crack tip damage zone of Blend 2. Crack tip blunting is observed.

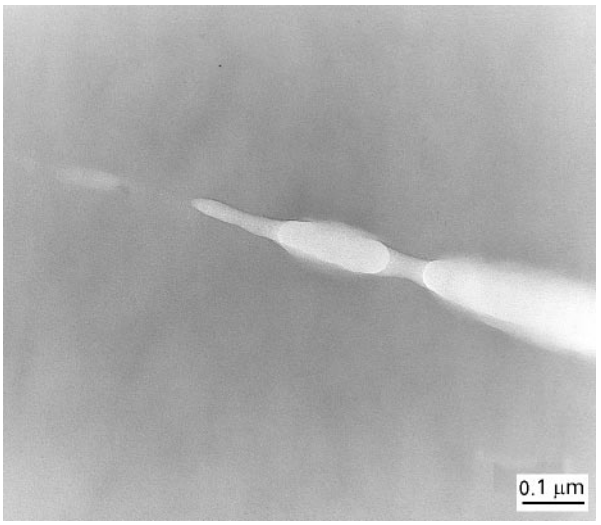

Figure 14 TEM micrograph taken at the DN-4PB crack tip damage zone of Blend 2. Crack tip blunting, crack segmentation, and crack bridging are observed.

in Blend 2 are likely to be highly localized ductile yielding of the matrix, crack tip blunting, crack bridging and crack segmentation.

The present study indicates that different formulations can help tailor the physical, mechanical and processing characteristics of the LCEs. For example, if the T_g and rigidity of the matrix is of concern, the rigid backbone epoxies, such as Tactix* 556 epoxy resin, should be utilized. To achieve better tack and drape properties plus latency of the resin, the tough epoxy formulation can be used [4]. For low temperature applications, a higher concentration of mesogenic segments in the LCE should be considered, e.g. Blend 1. For adhesive applications, epoxies with a high concentration of hydroxyl functional group should be mixed with the LCEs to improve the bonding with the metal surface. Also, from the morphological point of view, the LCEs can be explored and used either as a continuous matrix phase, as a co-continuous phase, or even as a filler phase, so long as the physical, mechanical, and processing properties as well as the economics of the blend are suitable for intended applications.

Finally, the effect(s) of LCE orientation in alteration of the physical and mechanical properties of the LCE blends has not yet been explored. This may further expand the application window for LCEs. This area is subject to future investigations.

4. Conclusions

The fracture toughness and failure mechanisms of LCE blends based on DGE-DHAMS are studied using SEN-3PB, DN-4PB, SEM, ROM, TOM and TEM techniques. Crack deflection, crack bifurcation, segmented cracking, crack bridging, and possibly, orientation/transformation toughening, are found to operate in Blend 1; while for Blend 2, where no observable LC domains are found, the crack path is straight. Matrix ductile yielding, crack tip blunting, crack bridging and crack segmentation are found to be the dominant toughening mechanisms for Blend 2. In the case of Blend 3, only limited crack tip yielding is observed. The use of formulating techniques to tailor the LCE physical, mechanical, and processing characteristics is found to be feasible for a wide range of applications.

Acknowledgements

The authors would like to thank E.I. Garcia-Meitin, N.A. Orchard, E.T. Vreeland, W.L. Huang, M.I. Villarreal, J.L. Bertram, C.C. Garrison, D.L. Barron and B.L. Burton for their support and discussion of this work.

References

1. H.-J. SUE, J. D. EARLS and R. E. HEFNER, Jr, *J. Mater. Sci.* (1996) in press.
2. J. D. EARLS and R. E. HEFNER, Jr and P. M. PUCKETT, US Patent 5,463,091, 1995.
3. J. D. EARLS and R. E. HEFNER, Jr and P. M. PUCKETT, US Patent 5,218,062, 1993.
4. J. L. BERTRAM, L. L. WALKER, J. R. BERMAN and J. A. CLARKE, US Patent 4,594,291, 1986.
5. G. C. BARCLAY, C. K. OBER, K. I. PAPATHOMAS and D. W. WANG, *J. Polym. Sci. Part A*: *Polym. Chem.* **30** (1992) 1831.
6. A. A. ROBINSON, S. G. McNAMEE, Y. S. FREIDZON and C. K. OBER, *Polymer Preprint* **34** (1993) 743.
7. Q. LIN, A. F. YEE, J. D. EARLS, R. E. HEFNER, Jr and H.-J. SUE, *Polym. Commun.* **35** (1994) 2679.
8. H.-J. SUE and A. F. YEE, *J. Mater. Sci.* **28** (1993) 2975.
9. H.-J. SUE, R. A. PEARSON, D. S. PARKER, J. HUANG and A. F. YEE, *Polymer Preprint* **29** (1988) 147.
10. H.-J. SUE, E. I. GARCIA-MEITIN and D. M. PICKELMAN, in "Elastomer technology handbook", edited by N. P. Cheremisinoff (CRC Press, Boca Raton, FL, 1993) p. 662.
11. H.-J. SUE, *Polym. Eng. Sci.* **31** (1991) 275.
12. O. L. TOWERS, "Stress intensity factor, compliance, and elastic η factors for six geometries" (The Welding Institute, Cambridge, UK, 1981).
13. ASTM standard, E399-81.
14. ASTM standard, E647-88a.
15. P. C. PARIS, in Proceedings of the 10th Sagamore Conference Syracuse, 1964, (Syracuse University Press, Syracuse, NY, 1964) p. 107.
16. A. S. HOLIK, R. P. KAMBOUR, S. Y. HOBBS and D. G. FINK, *Microstruct. Sci.* **7** (1979) 357.
17. J. KARGER-KOCSIS and K. FRIDRICH, *Colloid Polym Sci.* **270** (1992) 549.
18. H.-J. SUE, in preparation.
19. T.-Y. PAN, R. E. ROBERTSON and F. E. FILISKO, *J. Mater. Sci.* **24** (1989) 3635.
20. H.-J. SUE, J. L. BERTRAM, E. I. GARCIA-MEITIN, L. L. WALKER and J. W. WILCHESTER, *Colloid & Polym. Sci.* **272** (1994) 456.

Received 11 July
and accepted 23 October 1996